

Fuel Melting Simulation with FRAPCON/FRAPTRAN Codes for the Power-to-Melt-and-Maneuverability Simulation Exercise and Consideration of Model Modifications

Kenta Inagaki

To cite this article: Kenta Inagaki (2023): Fuel Melting Simulation with FRAPCON/FRAPTRAN Codes for the Power-to-Melt-and-Maneuverability Simulation Exercise and Consideration of Model Modifications, *Nuclear Technology*, DOI: [10.1080/00295450.2023.2239041](https://doi.org/10.1080/00295450.2023.2239041)

To link to this article: <https://doi.org/10.1080/00295450.2023.2239041>



Published online: 30 Aug 2023.



Submit your article to this journal



View related articles



View Crossmark data



Fuel Melting Simulation with FRAPCON/FRAPTRAN Codes for the Power-to-Melt-and-Maneuverability Simulation Exercise and Consideration of Model Modifications

Kenta Inagaki *

Central Research Institute of Electric Power Industry (CRIEPI), 2-6-1 Nagasaka, Yokosuka, Kanagawa 240-0196, Japan

Received October 17, 2022

Accepted for Publication July 17, 2023

Abstract — This paper presents simulation results of earlier fuel melting tests (*xM3* and *HBC4*) performed under the power-to-melt-and-maneuverability (P2M) simulation exercise organized within the Organisation for Economic Co-operation and Development (OECD)/Nuclear Energy Agency (NEA) framework for irradiation experiments. The simulations were performed using the single-rod performance analysis code FRAPCON/FRAPTRAN as a contribution of the Central Research Institute of Electric Power Industry (CRIEPI) to the P2M simulation exercise. To this end, the base irradiation of each sample was simulated using FRAPCON software, and the calculated result was used to define the initial state of the transient simulations; the *xM3* and *HBC4* ramp tests were simulated using FRAPTRAN. Fuel melting was not predicted for *xM3*, and the melting radius was underestimated for *HBC4* using the original version of FRAPTRAN. The value of the fuel/cladding gap conductance was modified to obtain results that satisfy the experimental measurement of the melting radius.

In this paper, the simulation results are compared with experimental results, and the causes for discrepancy between the simulation and experiment results are discussed. The necessary improvements for FRAPTRAN to achieve a better simulation of fuel melting are also discussed. These results can help calibrate codes against high-temperature behavior and improve fuel melting modeling toward the planned P2M power ramp tests.

Keywords — FRAPCON/FRAPTRAN, fuel melting, fuel performance simulation, fuel-cladding gap conductance.

Note — Some figures may be in color only in the electronic version.

I. INTRODUCTION

The Framework for Irradiation Experiments (FIDES) was formed in 2021 as an Organisation for Economic Co-operation and Development (OECD)/Nuclear Energy Agency (NEA) initiative for conducting irradiation programs on fuels and materials. In 2022, FIDES included 27 organizations from 12 countries that performed four joint experimental programs (JEEPs).^[1] The power-to-melt-and-maneuverability (P2M) exercise is an ongoing JEEP proposed by the Belgian Nuclear Research Center

(Belgium), the Commissariat à l’Energie Atomique et aux Energies Alternatives (France), and Electricité de France (France) to study the behavior of high-burnup fuel in light water reactors during slow- and high-power transients that lead to fuel melting without clad failure.

In P2M, a “simulation exercise on earlier fuel-melting experiments” is conducted by simulating previous power ramps, during which fuel melting has been observed, to calibrate codes against high-temperature behavior and improve fuel melting modeling toward the power ramp tests planned in P2M. The simulation exercise was performed by 13 organizations using 11 different fuel performance codes; their simulation results were

*E-mail: inagaki@criepi.denken.or.jp

gathered and compared to identify the modeling advancements needed to simulate fuel melting behavior.^[2]

The Central Research Institute of Electric Power Industry (CRIEPI) contributed to this simulation exercise by performing simulations using the single-rod performance analysis codes FRAPCON^[3] and FRAPTRAN.^[4] This paper presents detailed information on the setup and assumptions used in the CRIEPI simulations. Fuel melting was not reasonably predicted by the original version of FRAPTRAN; therefore, some modifications were made to the source code so that fuel melting occurred in the simulation. Since the purpose of the simulations performed in this research was not to correctly reproduce the test results but to investigate the limitation of existing codes and clarify the issues to be resolved, modifications were kept at a minimum.

The calculated and measured results were compared for validation purposes, and some discussions were conducted to clarify further issues to be improved for reasonably simulating fuel melting behavior using FRAPTRAN. In this paper, the details of the code and models used or modified to assess the fuel melting behavior are introduced in Sec. II. Input data and the results of the simulations of xM3 and HBC4 are presented in Secs. III and IV, respectively. Discussion of the results and the necessary improvement are given in Sec. V. Conclusions are presented in Sec. VI.

II. DESCRIPTION OF FRAPCON AND FRAPTRAN CODES

The FRAPCON4.0 and FRAPTRAN2.0 codes were developed within the framework of the reactor safety research program established by the U.S. Nuclear Regulatory Commission at the Pacific Northwest National Laboratory; they were used to simulate the fuel melting behavior in this study. FRAPCON was designed to evaluate the thermal and mechanical responses of a single fuel rod under normal operating conditions, whereas FRAPTRAN is used under transient conditions. In FRAPCON and FRAPTRAN, the fuel pellets, cladding, and surrounding coolant are considered, and the fuel pellets and cladding are modeled as a superposition of the one-dimensional axial and radial descriptions.

Finite difference or finite element methods with variable mesh spacing along the axial and radial directions are used for the pellet and cladding. The mechanical and thermal responses of a fuel rod are calculated from the given inputs that define the time profiles of the coolant condition and thermal power of the fuel pellets. Since

FRAPTRAN aims to target phenomena that occur in relatively short transient irradiation conditions, such as loss-of-coolant accidents and reactivity-initiated accidents, the axial growth, creep, and swelling of both the fuel and cladding are not considered in FRAPTRAN, as their effect is not significant over a short timeframe.^[4]

The base irradiation of the fuel rod samples used in the xM3 and HBC4 tests was simulated using FRAPCON; the simulation of the fuel melting ramp test was performed using FRAPTRAN. Some variables were calculated by FRAPCON and read by FRAPTRAN to define the initial state of the samples in the ramp tests; these included cladding oxide layer thickness, hydrogen concentration in the cladding, burnup distribution, total quantity of gas in the fuel rod free volumes and gas composition, permanent deformation of fuel and cladding, fuel relocation displacement, amount of fission gas at grain boundaries, and fuel swelling after the base irradiation period.

In FRAPTRAN, users must select a model from several suboptions to reasonably evaluate the behavior of pellet deformation, fuel relocation, fission gas release (FGR), deformation and chemical reactions of cladding and coolant, depending on the conditions. In all calculations introduced in this paper, the following suboption was selected: the pellet radius evolution was calculated from the radial thermal expansion of each ring of the fuel pellet mesh. The model used in FRAPCON-3.3^[5] was selected for fuel relocation. The FGR was evaluated using the transient gas release model initialized with the FRAPFGR model in FRAPCON-4.0.^[3] For cladding oxidation, the “cathca” suboption was selected where the Cathcart correlation is used for the metal-water reaction.^[4] The Fracases-I model was used to calculate the deformation of the fuel and cladding.^[4]

II.A. Modeling for Fuel Melting in FRAPTRAN

In FRAPTRAN, the melting of UO_2 fuel is evaluated using a single melting temperature, whereas the liquidus and solidus temperatures are defined for the mixed-oxide fuel based on the Pu content. The melting temperature of UO_2 is dependent on burnup (Fig. 1a); this correlation has been validated for burnups up to 62 GWd/tonne U.^[4] Although recent experimental measurements have revealed the dependency of the melting temperature on the stoichiometry of UO_{2-x} ,^[6] this has not been considered. The conservative estimate of uncertainty is ± 50 K; for temperatures greater than 2 K below melting, the molten fraction and latent heat of fusion are used to

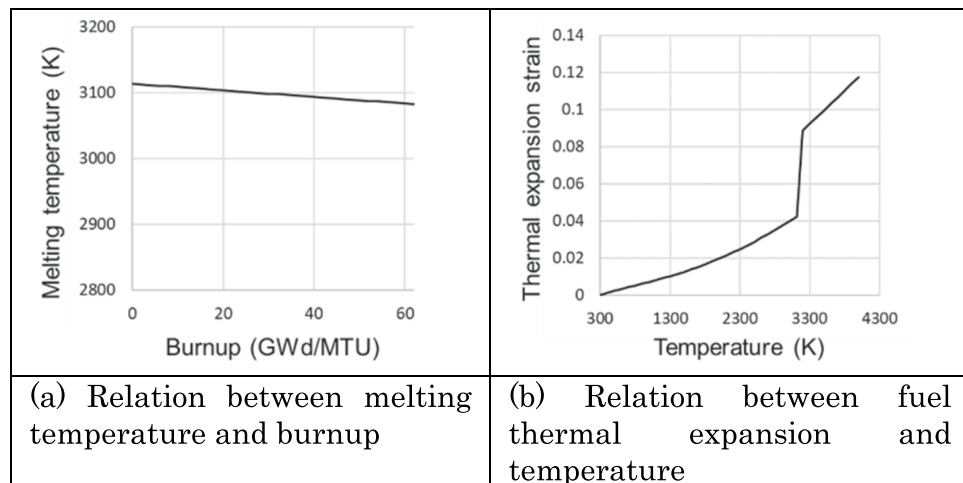


Fig. 1. Correlations of the material properties used in FRAPTRAN.

interpolate the enthalpy of solid fuel and just-melted fuel at the melting temperature.^[7]

The thermal conductivity of the UO₂ fuel was evaluated as a function of density, burnup, and temperature; the validity of the correlation was confirmed for the range between 300 and 3000 K and up to 62 GWd/tU. Above 3000 K, the same correlation for the solid phase was used, although the uncertainty was considered large.^[7] Although the effect of deviation from stoichiometry x in UO_{2+x} on the thermal conductivity has been confirmed,^[8] it was not considered in the model used.

The specific heat capacity of molten UO₂ fuel was assumed to be constant at 503 J/kg·K,^[9] and that of the solid-state fuel was dependent on temperature. This correlation is valid for temperatures from 300 K to more than 4000 K, with a standard error of ± 3 J/kg·K.^[7]

The thermal expansion of the fuel was calculated as a function of temperature and considered the fraction of molten fuel as shown in Fig. 1b. An expansion equal to a linear strain of 0.043 was added when melting occurred; this corresponded to the steep increase in volume caused by liquefaction.^[7]

Fuel melting does not affect the fission-gas release behavior in FRAPTRAN because the transient fission-gas release model is as follows: all grain boundary gases are released when the temperature exceeds 1366 K and a part of the gas in the grains is released at 2089 K, which indicates that the gas release occurs below the melting temperature. These threshold temperatures were determined so that the measured release values in NSRR and CABRI tests were well predicted.^[10] Although a central hole was observed in both the xM3 and HBC4 test samples,^[2] the formation of a central hole in the fuel is not modeled in FRAPTRAN-2.0. The models for porosity

migration and central void formation have been implemented in FRAPCON-EP^[11] by Andrew, but they have not been implemented in the current versions (FRAPCON-4.0 and FRAPTRAN-2.0). More detailed information on the mechanical property correlations and models for fuel melting have been reported in the literature.^[7]

II.B. Code Modifications in FRAPTRAN for the xM3 and HBC4 Simulations

Three code modifications were performed to obtain reasonable results in the simulations of the xM3 and HBC4 fuel melting tests, as summarized in Table I. Since the purpose of the calculations performed in this research was to investigate the limitation of FRAPTRAN for fuel melting simulation rather than correctly reproducing the test results, the modifications were based on simple assumptions to investigate their effect.

The first modification was related to the thermal transport model. The fuel centerline temperature was underestimated by the original version of FRAPTRAN-2.0,

TABLE I
FRAPTRAN Code Modification for the xM3 and HBC4 Simulations

Description	Remarks
Gap heat conductance between fuel and cladding	Multiplier introduced.
Fuel melting	Invalidated.
Nonslip condition at clad/fuel interface	Invalidated.

which indicated no fuel melting, and it conflicted with measurement results wherein fuel melting was clearly indicated in the Post-Irradiation Examination (PIE) results of the xM3^[12] and HBC4^[13] samples after the ramp test. The underestimation of the fuel centerline temperature indicated the overestimation of energy transport from the fuel to the outside, and this comprised heat transport within the fuel pellet and cladding and the heat transfer at the fuel/cladding gap and cladding/coolant interface. Among these, the heat transfer at the fuel/cladding gap (referred to as the gap heat conductance) was a complex mechanism that involved fill gas conductance, thermal radiation, and solid contact conductance, and had large uncertainty because of several factors, such as the inaccurate estimation of contact characteristics, difficulties in estimating the temperature jump over the gap distance and gas conductance property, and an insufficient description of the appropriate heat transfer regime.^[14] Although the recent improvement in the gap conductance model succeeded in reducing the errors,^[14,15] they have not been equipped in FRAPTRAN. Therefore, a multiplier was introduced in the FRAPTRAN source code to obtain reasonable calculation results based on the assumption that the gap heat conductance at the fuel/cladding is the main cause of the discrepancy.

The second modification concerned the fuel melting flag in FRAPTRAN. The test calculations indicated that the FRAPTRAN calculation stopped unintentionally when fuel melting occurred in the simulation because of the numerical convergence problem; this was attributed to the expansion of the molten fuel caused by the increase in volume in the liquefied part of the pellet. No convergence was obtained for the cladding deformation calculation due to an excessively large strain as FRAPTRAN tends to overpredict the fuel-cladding mechanical interaction.^[4] The source code of FRAPTRAN was modified to invalidate the fuel melting flag to avoid this convergence problem. In addition, the melting radius was evaluated by counting the number of fuel nodes at which the local temperature reached the melting temperature threshold. For the sake of simplicity, the temperature threshold for melting was defined as $T_m = 3120$ K, which is independent of burnup.

The third and last modifications were related to the contact condition between the fuel pellets and cladding. The test calculations confirmed that the axial elongation of the cladding during the ramp test was overestimated, as shown in Fig. 5b, for the xM3 irradiation; this was attributed to a nonslip condition that was assumed when the fuel and cladding were in contact. The source code of FRAPTRAN was modified such that the free-slip

condition was implemented to quantitatively estimate the effect of the nonslip condition.

III. SIMULATIONS OF xM3

III.A. xM3 Base Irradiation Simulation

III.A.1. xM3: Inputs

A FRAPCON simulation was performed to evaluate the effect of base irradiation on the xM3 sample. Only a part of the irradiated father rod was used in the xM3 ramp test; this part was referred to as segment-4. The simulation of the full-length father rod was performed first to evaluate the coolant temperature condition around segment-4 because the FRAPCON and FRAPTRAN simulations must be performed with an identical sample size; then, the calculation of segment-4 was performed. The parameters and irradiation conditions used in the FRAPCON simulation of segment-4 are summarized in Table II and presented in Fig. 2.

The 441-mm-long sample was axially divided into 10 nodes. The power history during the two-cycle irradiation was defined by the time profile of the average linear heat generation rate (Fig. 2a) and the ratio of linear power along the axial direction (Fig. 2b). In the full-length father-rod calculation, the coolant temperature at the lower edge of segment-4 was evaluated as 581 K. Therefore, the inlet temperature of the segment-4 calculation was set as 581 K. The value of the mass flux of the coolant around the fuel was adjusted as shown in Fig. 2c such that the evaluated coolant outlet temperature was equal to the value from the full-length calculation; this helped reduce the source of uncertainty in the simulation.

III.A.2. xM3: Results

The results of the base irradiation simulation of the xM3 sample are summarized in Table III and Fig. 3. The fuel stack length, average fuel rod burnup, and average fast fluence of the fuel rod, which were obtained at the end of life (EOL) by the FRAPCON calculation, agreed well with the measurement. The FGR ratio of the xM3 sample was evaluated to be 0% in this calculation. In the FRAPFGR model, which was used in this calculation for the FGR analysis, the amount of gaseous fission products (FPs) inside the grain and that at the grain boundary were calculated at each time step; some of them were released outside the pellet when the gas concentration at the grain boundary exceeded the threshold value.

TABLE II
Parameters for the Base Irradiation Simulation of Segment-4 of the xM3 Sample

Parameter Name	Description	Value	Remarks
Numerical			
na nr	Number of equal-length axial nodes Number of equal-area radial nodes in the fuel	10 17	— —
Fuel Rod			
Dco Thkclad Thkgap Totl Cpl Den Icm Fgpav	Cladding outer diameter (mm) Cladding wall thickness (mm) Pellet-cladding as-fabricated radial gap thickness (mm) Total fuel column length (mm) Cold plenum length (mm) As-fabricated apparent fuel density (%) Cladding type Initial fill gas pressure (MPa)	9.5 0.57 0.085 441 44 95.3 ZIRLO 2	— — — — — — — —
Power			
qmpy qf	Linear heat generation rate (kW/m) Ratio of the linear power	See Fig. 2a. See Fig. 2b.	— —
Coolant			
tw p2 go	Coolant inlet temperature (K) Coolant system pressure (MPa) Mass flux of coolant around fuel rod	581 15.7 See Fig. 2c.	Evaluated by full-length calculation. — Adjusted on the basis of the full-length calculation.

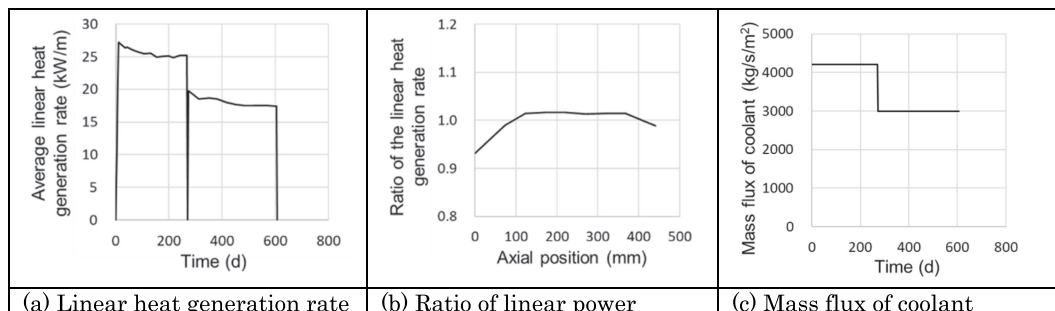


Fig. 2. Parameter profiles for the base irradiation simulation of the xM3 sample (segment-4).

In this study, the default value in FRAPCON was used for the threshold. The FP gas concentration in the grain boundary did not grow above the threshold because the xM3 father rod was irradiated for only two cycles, which resulted in 0% FGR. The evaluated values of 8 to 11 μm for the oxide layer thickness on the cladding outer surface were reasonable compared with the measured value of 5 to 11 μm .^[12]

Figure 3a shows the evaluated axial profile of the cladding diameter after base irradiation along with the measurement results. Although FRAPCON slightly underestimated the values, they were satisfactory because the differences were less than 10 μm . The axial profile of the residual radial gap at EOL was evaluated as shown in Fig. 3b. Only the evaluated results are shown because no measurement data were available. They are almost flat

TABLE III
Comparison of Evaluated and Measured Values for the xM3 Base Irradiation

Time	Description	Simulation (FRAPCON)	Measurement
EOL	Fuel stack length (mm)	443	443
EOL	Average fuel rod burnup (MWd/kgU)	26.7	27
EOL	Average fast fluence of the fuel rod (n/m^2)	4.45×10^{25}	4.39×10^{25}
EOL	FGR ratio	0	—
EOL	Oxide layer thickness on outer surface (μm)	8 to 11	5 to 11

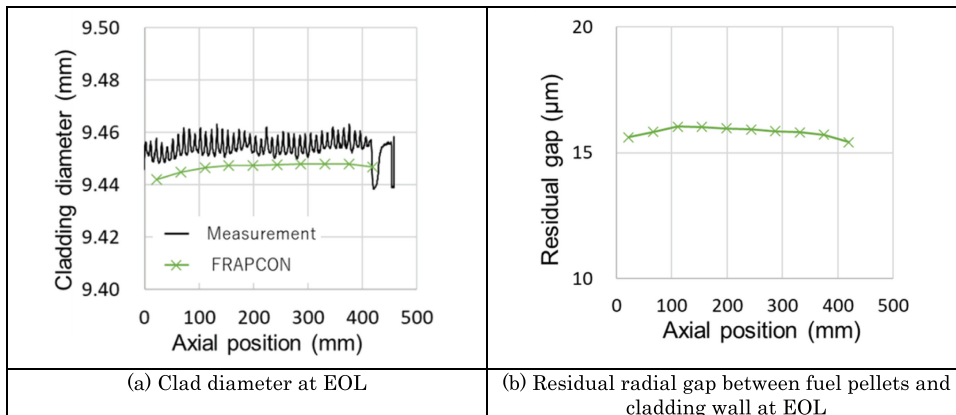


Fig. 3. Axial profiles calculated by FRAPCON for the xM3 base irradiation.

along the axial direction because segment-4 was located near the middle of the father rod; the heat generation rate and temperature were not strongly dependent on the axial position, as shown in Fig. 2b.

The validity of the base irradiation simulation result was confirmed, and it was used to define the initial state of the sample in the ramp test.

III.B. xM3 Ramp Test Simulation

III.B.1. xM3 Ramp Test: Inputs

The parameters used for the simulation of the xM3 ramp test are listed in Table IV and shown in Fig. 4. The sample was axially divided into 10 nodes, as well as the FRAPCON calculation. The fuel and cladding were radially discretized with 41 and 5 meshes, respectively.

The parameters of the fuel rod design were determined based on the actual configuration of the sample. The axial profiles of the cladding diameter, fuel cladding gap, and pellet diameter, which were calculated in the base irradiation simulation with FRAPCON, were read by FRAPTRAN to re-initialize the sample state. The gap heat conductance between the fuel and cladding was

manually reduced so that the fuel pellet temperature exceeded the melting temperature within the measured melted fuel radius at the ramp terminal level (RTL). The value of the multiplier for gap heat conductance was set to 0.075.

The time history of the linear heat generation rate was given by the input, as shown in Fig. 4a; its axial profile is set as shown in Fig. 4b, which was based on the actual test conditions.^[12]

Since the coolant flows from the top to the bottom in the R2 ramp rig, the coolant temperature was set higher at a lower position, as shown in Fig. 4c. The “heat” option was used, which was installed in FRAPTRAN to specify the specific thermal-hydraulic conditions to deal with this condition in the simulation. Using the heat option, the axial distribution of the coolant temperature was prescribed as shown in Fig. 4c, instead of calculating the coolant temperature distribution. The value of the heat transfer coefficient between the cladding and coolant was determined on the basis of the cladding surface temperature measured in the xM3 test. By setting the heat transfer coefficient to be 70 000 W/m²/K/s, the calculated cladding surface temperature at the RTL met the measured value of 620 K.

TABLE IV
Parameters for the Ramp Test Simulation of xM3

Parameter Name	Meaning	Value	Remarks
Numerical			
naxn	Number of equal-length axial nodes	10	—
nfmesh	Number of equal-width radial nodes in the fuel	41	—
ncmesh	Number of equal-area radial nodes in the cladding	5	—
Fuel Rod			
rodLength	Initial fuel pellet stack length (mm)	441	—
RodDiameter	Cladding outer diameter (mm)	—	Re-initialized with FRAPCON results.
gapthk	Radial fuel-cladding gap thickness (mm)	—	Re-initialized with FRAPCON results.
vplen	Plenum volume (m^3)	2.4E-6	—
FuelPelDiam	Fuel pellet diameter (mm)	—	Re-initialized with FRAPCON results.
frden	Fractional theoretical density	0.953	—
roughf	Arithmetic mean roughness of fuel pellet surface (μm)	3	—
CladType	Cladding type	ZIRLO	—
Gappf0	As-fabricated fill gas pressure (MPa)	2	—
Tgas0	As-fabricated fill gas temperature (K)	300	—
—	Multiplier on gap heat conductance	0.075	Adjusted.
Power			
RodAvePower	Average and maximum linear heat generation rate	See Fig. 4a.	—
AxPowProfile	Axial power profile	See Fig. 4b.	—
Coolant			
htca	Heat transfer coefficient between the clad and coolant ($\text{W}/(\text{m}^2 \cdot \text{K})$)	70 000	Adjusted.
Pbh2	Coolant pressure (MPa)	14.7	—
tblka	Coolant temperature	See Fig. 4c.	—

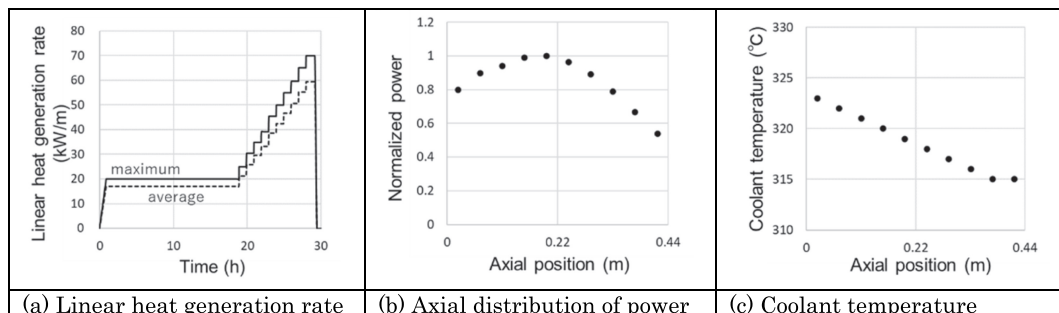


Fig. 4. Parameter profiles for the ramp test simulation of xM3.

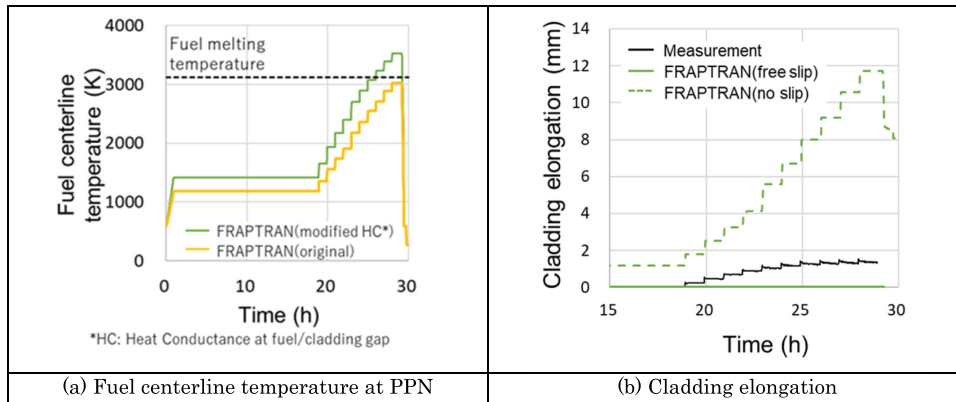


Fig. 5. Time profiles calculated by FRAPTRAN for the xM3 ramp test.

III.B.2. xM3 Ramp Test: Results

The FRAPTRAN simulation results of the xM3 ramp test are summarized in Table V and Fig. 5. The fuel stack length after the ramp test was evaluated to be 443 mm, which was the same as the FRAPCON result (Table III). This indicated that there was no additional fuel expansion during the ramp test. This was attributed to the fact that densification, the gaseous swelling, and the solid swelling were not considered in FRAPTRAN.^[4] The evaluated FGR rate was 4.3%, whereas the measured FGR was approximately 34%. The reason for this underestimation must be investigated in the future to improve the simulation accuracy because the FGR strongly affects the mechanical and thermal performance of the fuel rods, especially in transient scenarios. The volume of the released gas, internal pressure, and internal free volume are measured and compared in Table V. The pressure and released gas volume were underestimated, and the internal free volume was predicted reasonably. These results are consistent with the fact that FGR was underestimated by FRAPTRAN.

The evaluated time profile of the fuel centerline temperature at the peak power node (PPN) is shown in Fig. 5a,

where the solid yellow line is the result of the simulation performed with the original FRAPTRAN; the solid green line was obtained by the model with modified gap heat conductance. As clearly indicated in the figure, the original FRAPTRAN did not predict the melting of fuel. Fuel melting was reached by using the reduced gap heat conductance.

The time profile of the cladding elongation is shown in Fig. 5b; the dotted green line represents the result of the simulation performed under the no-slip condition, which is the original model of FRAPTRAN, and the solid green line represents the modified code where the free-slip condition was assumed. Both results were obtained by the calculation with the reduced gap heat conductance. A large axial strain comparable to the fuel stack axial strain caused by thermal expansion was obtained on the cladding when the no-slip condition was assumed because the fuel and cladding were in contact during the power ramp period. This resulted in a large discrepancy between the calculations and measurements. The axial elongation of the cladding was evaluated to be as small as 0.02 mm when the free-slip condition was assumed. The results of the free-slip condition were reported for a simulation exercise^[2]; these results indicated the necessity for

TABLE V
Comparison of Evaluated and Measured Values for the xM3 Ramp Test

Time	Description	Simulation (FRAPTRAN)	Measurement
EOL	Fuel stack length (mm)	443	—
EOL	FGR ratio (%)	4.3	34
EOL	Released gas volume, 0.1 MPa, 0°C (cm ³)	7.7	56.2
EOL	Internal pressure, 0°C (MPa)	2.14	3.48
EOL	Internal free volume (cm ³)	3.37	3.65

models that can reasonably deal with the mechanical interaction between the fuel and cladding that are in contact by considering the local frictional force.

The axial profiles obtained by FRAPTRAN are shown in Figs. 6a through 6d. FRAPTRAN predicted the cladding diameter profile, but slightly underestimated it, as indicated in Fig. 6a; the cladding failure was not predicted. The diameters of the pellets after the ramp test are illustrated in Fig. 6b. Although the difference in power at the middle and at the edge of the fuel stack was significant (Fig. 4b), the calculated fuel stack profile was almost flat because no additional deformation of pellets was considered in FRAPTRAN except for thermal expansion. The pellet diameter was evaluated to be lower than the measurement because the calculations were allowed to simulate fuel melting (Fig. 5a), but the additional fuel strain due to fuel liquefaction was neglected.

Figures 6c and 6d show the axial distributions of the fuel centerline temperature and melted fuel radius at RTL, respectively. The calculated melted fuel radius agreed well with the measurements because the gap heat conductance was adjusted to obtain this result, as shown in Fig. 6d. Two additional simulation cases are shown in the figures, where the power was changed by $\pm 5\%$ to account for the power uncertainty. The melted radius increased by 17% at $+5\%$

power, and it decreased by 25% at -5% power. Although a central hole was formed in the xM3 sample,^[12] it was not predicted because FRAPTRAN is currently not equipped with a model to evaluate the central hole formation.

IV. SIMULATIONS OF HBC4

IV.A. HBC4 Base Irradiation Simulation

IV.A.1. HBC4: Inputs

A FRAPCON simulation was performed to evaluate the effect of base irradiation on the HBC4 sample. The parameters are listed in Table VI and Fig. 7; the size and material properties of the samples were defined based on the actual sample properties. The power history during the three-cycle irradiation was defined by the time profile of the average linear heat generation rate (Fig. 7a) and the ratio of linear power along the axial direction (Fig. 7b). For the coolant condition, the mass flux of the coolant was determined (Fig. 7c) by multiplying the measured channel velocity (2.77 m/s) by the water density of 791 kg/m^3 , which was a measured value of the water at 14 MPa and 262.5°C .

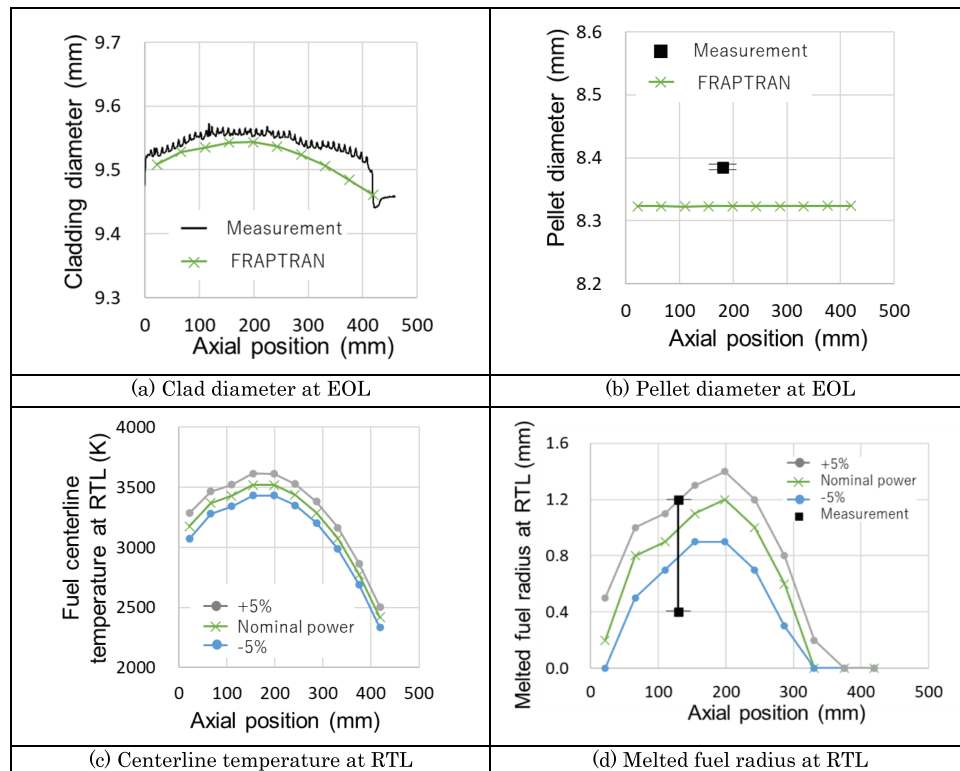


Fig. 6. Axial profiles calculated by FRAPTRAN for the xM3 ramp test.

TABLE VI
Parameters for Base Irradiation Simulation of HBC4

Parameter Name	Description	Value	Remarks
Fuel Rod			
Dco	Cladding outer diameter (mm)	9.5	—
Thkcll	Cladding wall thickness (mm)	0.63	—
thkgap	Pellet-cladding as-fabricated radial gap thickness (mm)	0.098	—
totl	Total fuel column length (mm)	996.3	—
cpl	Cold plenum length (mm)	94.7	—
den	As-fabricated apparent fuel density (%)	94.4	—
icm	Cladding type	Zircaloy-4	—
fgpav	Initial fill gas pressure (MPa)	2	—
Power			
qmpy	Linear heat generation rate (kW/m)	See Fig. 7a.	—
qf	Ratio of the linear power	See Fig. 7b.	—
Coolant			
tw	Coolant inlet temperature (K)	528	—
p2	Coolant system pressure (MPa)	14.2	—
go	Mass flux of coolant around fuel rod	See Fig. 7c.	Determined by multiplying the measured channel velocity by the water density.

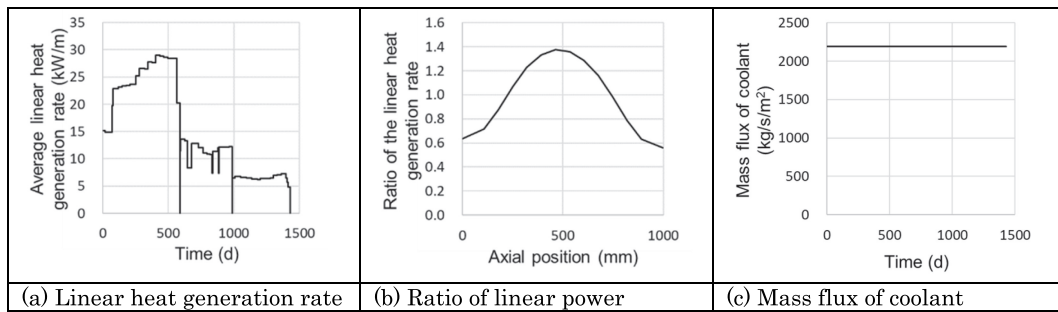


Fig. 7. Parameter profiles for base irradiation simulation of HBC4.

IV.A.2. HBC4: Results

The results of the base irradiation simulation of HBC4 are summarized in Table VII and Fig. 8. The fuel stack length and average fuel rod burnup evaluated by FRAPCON were in good agreement with the measurement, whereas the average fast fluence of the fuel rod was not compared because of the absence of measurement data. For the FGR, FRAPCON predicted 7.5%, whereas 5.3% was measured in the sibling sample at 43.7 GWd/tU. The FGR prediction for HBC4 was within the standard deviation because the reported standard deviation for steady-state predictions was 2.6% of the absolute value.^[16]

The axial profile of the cladding diameter after base irradiation is shown in Fig. 8a. During irradiation, the cladding is under compression because of the high coolant pressure. FRAPCON analysis revealed that the cladding experienced circumferential compressive plastic strain, which was more significant in the middle of the fuel rod because the temperature was high. Consequently, the cladding diameter remained larger at both ends of the stack. This behavior was correctly reproduced using FRAPCON. However, the W-shaped profilometries were calculated, and this was not confirmed by the measurements. This was caused by overpredicting the swelling of the fuel pellets. The calculated cladding diameter was considered

TABLE VII
Comparison of Evaluated and Measured Values for HBC4 Base Irradiation

Time	Description	Simulation (FRAPCON)	Measurement
EOL	Fuel stack length (mm)	1003	1002
EOL	Average fuel rod burnup (MWd/kgU)	48.2	47
EOL	Average fast fluence of the fuel rod (n/m^2)	7.98×10^{25}	—
EOL	FGR ratio (%)	7.5	5.3 (43.7 GWd/tU)
EOL	Oxide layer thickness on outer surface (μm)	2 to 13	—

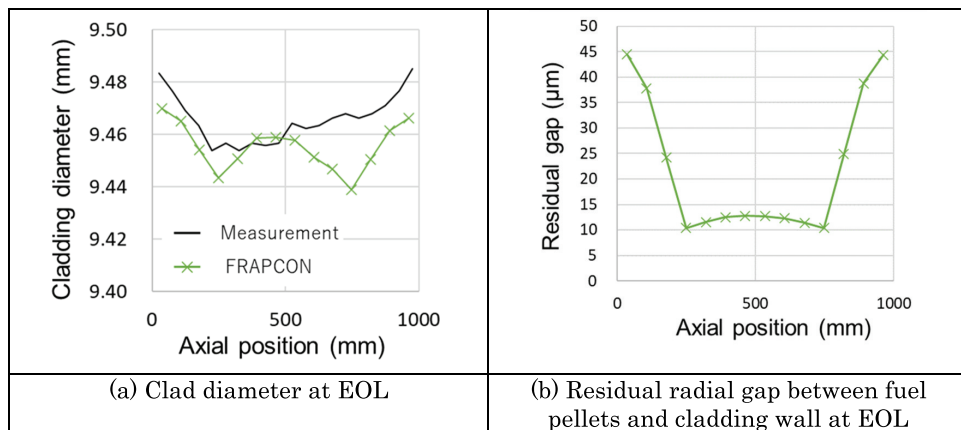


Fig. 8. Axial profiles calculated by FRAPCON for the HBC4 base irradiation.

reasonable because the error was less than 30 μm , except for the overestimation of the diameter increase at the pin midplane caused by contact with the pellets.

A larger gap remained at both ends because the cladding compression was less significant (Fig. 8b). A constant gap of around 10 μm remained at the midplane like a plateau. In this region, the gap had been closed during irradiation, and a gap of about 10 μm was formed when the fuel rod was removed from the reactor and cooled because there was no longer thermal expansion in the fuel pellets. These FRAPCON calculation results were used in the FRAPTRAN simulation.

IV.B. HBC4 Ramp Test Simulation

IV.B.1. HBC4 Ramp Test: Inputs

The parameters used for the simulation of the HBC4 ramp tests are summarized in Table VIII and Fig. 9. A 1002-m-long sample was axially divided into 14 nodes, whereas the fuel and cladding were radially discretized with 40 and 5 meshes, respectively. The parameters of the

fuel-rod design were determined based on the actual configuration of the sample. The axial profiles of the cladding diameter, fuel cladding gap, and pellet diameter were calculated in the base irradiation simulation of FRAPCON; they were read by FRAPTRAN to re-initialize the sample state. The gap heat conductance between the fuel and cladding was reduced from the value calculated using the original FRAPTRAN model by multiplying the value by 0.2. Although the modified value of the gap heat conductance was closer to the original FRAPTRAN model compared to the xM3 case, it was still necessary to modify the gap heat conductance to obtain a reasonable value on the basis of the experimental value of the molten fuel radius.

The time history of the linear heat generation rate was given by the input, as shown in Fig. 9a; its axial distribution was set as shown in Fig. 9b to simulate the actual power profile in the ramp test. The coolant temperature was kept constant along the axial direction, as shown in Fig. 9c, because the pressurized water capsule device in the BR2 reactor was used for the HBC4 ramp test as a stagnant water testing capsule. The heat transfer coefficient between the cladding and coolant was set again to 70 000 W/m²/K/s, as in the xM3 simulation.

TABLE VIII
Parameters for the Ramp Test Simulation of HBC4

Parameter Name	Description	Value	Remarks
Numerical			
naxn nfmesh	Number of equal-length axial nodes Number of equal-width radial nodes in the fuel	14 40	— —
ncmesh	Number of equal-area radial nodes in the cladding	5	—
Fuel Rod			
rodLength RodDiameter	Fuel pellet stack length (mm) Cladding outer diameter	996.3 —	— Re-initialized with FRAPCON results.
gapthk	Radial fuel-cladding gap thickness	—	Re-initialized with FRAPCON results.
vplen FuelPelDiam	Plenum volume (m^3) Fuel pellet diameter	5.05E-6 —	— Re-initialized with FRAPCON results.
frden roughf	Fractional theoretical density Arithmetic mean roughness of fuel pellet surface (μm)	0.944 3	— —
CladType Gappr0 Tgas0 —	Cladding type As-fabricated fill gas pressure (MPa) As-fabricated fill gas temperature (K) Multiplier on gap heat conductance	Zircaloy-4 2 300 0.2	— — — Adjusted.
Power			
RodAvePower	Average and maximum linear heat generation rate	See Fig. 9a.	—
AxPowProfile	Axial power profile	See Fig. 9b.	—
Coolant			
htca Pbh2 tblka	Heat transfer coefficient between the cladding and coolant ($\text{W}/(\text{m}^2 \cdot \text{K})$) Coolant pressure (MPa) Coolant temperature	70 000 14.2 See Fig. 9c.	Adjusted. — —

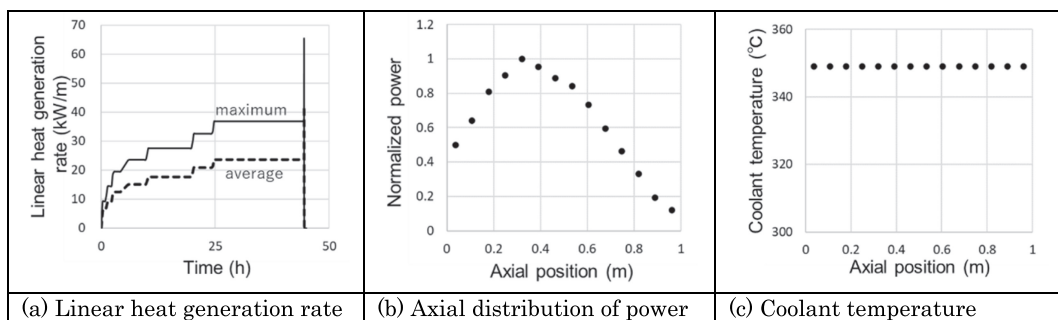


Fig. 9. Parameter profiles for the ramp test simulation of HBC4.

IV.B.2. HBC4 Ramp Test: Results

The fuel stack length was predicted to be 1003 mm, which was like that evaluated by FRAPCON for the base irradiation simulation. No additional deformation of the fuel was considered, except for the thermal deformation in FRAPTRAN. Only values evaluated by FRAPTRAN are listed in **Table IX** because the measured data for the internal gas after base irradiation were not obtained for the HBC4 sample.

The time profiles of the centerline temperature and cladding elongation obtained from the FRAPTRAN simulation are presented in **Fig. 10a**. The centerline temperature predicted by the original FRAPTRAN model was slightly higher than the melting temperature, as indicated by the dashed line. The melted radius evaluated by the original FRAPTRAN was considerably smaller than the measured value (0.8 to 1.1 mm at an axial position of 337 mm from the bottom of the fissile column (BFC), and 0.2 to 0.8 mm at 365 mm/BFC); a multiplier of 0.2 was used to reduce the gap heat conductance between the fuel and cladding.

Although the cladding elongation after the ramp test was not measured for HBC4, the cladding elongation evaluated using FRAPTRAN is plotted in **Fig. 10b** for

both the free-slip and no-slip cases. Similar to the xM3 results, an excessively large cladding elongation was predicted by the no-slip model, whereas the free-slip model predicted an almost zero elongation.

The evaluated and measured axial profiles of the cladding diameter after the ramp test are compared in **Fig. 11a**. A large discrepancy was observed in the cladding failed region, wherein several large peaks related to cladding cracks were measured, and FRAPTRAN did not predict cladding failure. Except for the failed regions, FRAPTRAN reasonably evaluated the cladding diameter.

Figures 11b and **11c** show the axial distributions of the fuel centerline temperature and melted fuel radius at RTL, respectively. Melting occurred at 200 to 600 mm/BFC for the nominal power case, which may be overestimated because no melting was observed in the PIE of the fuel cross section at an axial position of 559 to 565 mm/BFC. This indicated that the calibration of the gap heat conductance was not sufficient to explain the discrepancy between the measurement and simulation results. Two additional cases are shown in the figures, where the power was changed by $\pm 7\%$ to account for power uncertainty. The melted radius increased by 30% at +7% power and decreased by 30% for the -7%

TABLE IX
Comparison of Evaluated and Measured Values for the HBC4 Ramp Test

Time	Description	Simulation (FRAPTRAN)	Measurement
EOL	Fuel stack length (mm)	1003	1002
EOL	FGR ratio (%)	7.4	—
EOL	Released gas volume, 0.1 MPa, 0°C (cm^3)	50.9	—
EOL	Internal pressure, 0°C (MPa)	3.9	—
EOL	Internal free volume (cm^3)	6.24	—

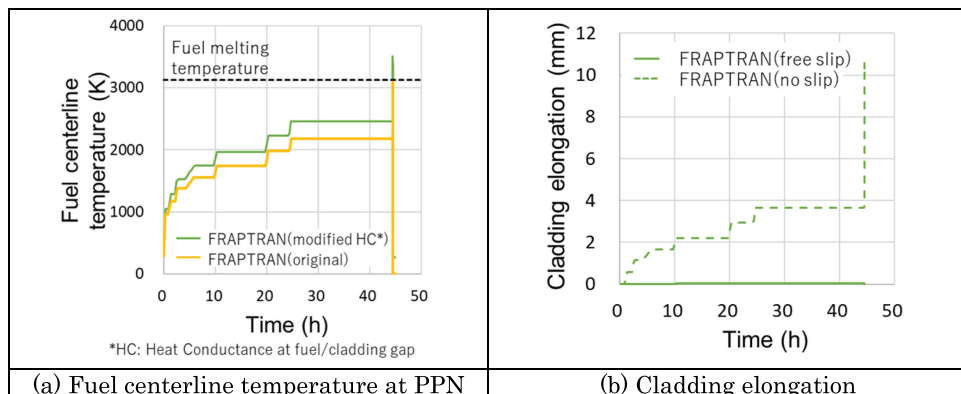


Fig. 10. Time profiles calculated by FRAPTRAN for the HBC4 ramp test.

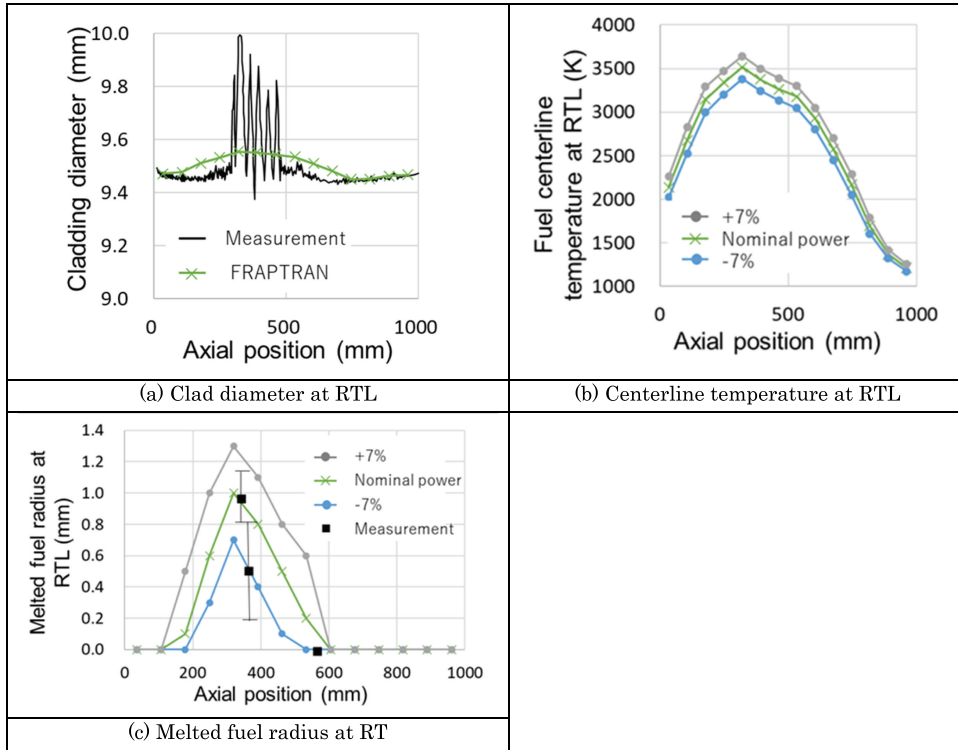


Fig. 11. Axial profiles calculated by FRAPTRAN for the HBC4 ramp test.

case. Although a central hole was observed in the HBC4 sample,^[13] as in the xM3 sample, no model was equipped in FRAPTRAN to predict its formation.

V. ANALYSIS AND DISCUSSION

A reasonable fuel melting radius at the PPN was not calculated using the original FRAPTRAN but was obtained by reducing the gap heat conductance at the fuel/clad interface. Since the gap heat conductance was only one of many factors to be considered to explain the reason for the centerline temperature underestimation, it was difficult to validate the value of the multiplier (0.075 for xM3 and 0.2 for HBC4). However, the necessary improvements of the FRAPTRAN models were clarified by investigating these calculation results as follows.

In FRAPTRAN, the gap heat conductance at the fuel/clad interface comprised three components: heat transfer through the fuel-cladding solid-solid contact, heat radiation, and heat conduction through the gas in the fuel-cladding gap. The simulation results obtained by the original FRAPTRAN confirmed that the amount of energy transferred through the gap gas was dominant among the three factors under the xM3 and HBC4 test conditions. The gap gas conductance was evaluated based on the heat transfer coefficient h_{gas} , which is determined by

$$h_{gas} = \frac{K_{gas}}{x_{gap} + x_{jump}} , \quad (1)$$

where K_{gas} represents the gas thermal conductivity; x_{gap} represents the distance of the gas gap where a minimum value is defined as the maximum between the summation of the fuel surface roughness R_c and the cladding surface roughness R_c or 1.27×10^{-7} m; and x_{jump} represents the combined fuel and cladding temperature jump distance, which accounts for the temperature discontinuity on the fuel and cladding surfaces.^[4] The gap heat conductance is strongly dependent on the gap distance; therefore, one possible reason for the discrepancy between the simulation and measurement results for xM3 and HBC4 was that the gap distance was underestimated.

Another reason for the excessively high conductance was that the evaluated value of the thermal conductivity K_{gas} in Eq. (1) is a function of the gas composition. The thermal conductivity of fission gases, such as xenon and krypton, is lower than that of helium. However, the reduction in the gas thermal conductivity caused by the released fission gas was not correctly evaluated because FGR was underestimated for xM3, as listed in Table V. In either case, an improved model for the evaluation of gap properties should be developed for a better prediction of the thermal response under fuel melting conditions.

Furthermore, because a large discrepancy was observed in the evaluated gap distance among the different codes involved in the OECD/NEA-FIDES benchmark activity,^[2] improving the gap distance prediction is also an important task to improve the calculation of the fuel melting behavior.

Another challenge in applying FRAPTRAN for the simulation of the fuel melting behavior is the estimation of cladding deformation. As described in reference,^[4] it is assumed in the FRAPTRAN simulation that the cladding follows the fuel dimensional changes from fuel thermal expansion and fuel melting when the fuel-cladding gap is closed. Furthermore, it was assumed that there was little fuel creep or compliance, which resulted in an overprediction of the fuel-cladding mechanical interaction strain for some transients with high fuel centerline temperatures (>2300 K) because some fraction of the fuel expansion may be accommodated by dishes, which will not contribute to fuel-cladding mechanical interaction strains. Therefore, the cladding deformation was always overpredicted, or a convergence problem occurred when fuel melting was simulated.

In addition to these, modifications of the models for the following phenomena are critical to the adequate prediction of fuel melting behavior during transient conditions:

1. Central hole formation in the fuel pellet affects both the thermal and mechanical behavior of the fuel. It is important to implement a model that can predict the central void formation^[11,17] for the simulation of fuel that is exposed to very high temperatures.

2. Thermal property modeling for the high-temperature region (more than 3000 K) in FRAPTRAN has a large uncertainty and it might reduce the reliability of the simulation results when fuel melting occurs. In the latest studies, molecular dynamics simulations are used to estimate the thermal properties of UO₂ at high temperatures.^[18,19] Introducing these findings should improve the simulation of fuel melting behavior.

3. The FGR model also affects both the mechanical and thermal behavior because fuel pellet expansion is dependent on the amount of fission gas left in the pellet and the size of the pellet affects the heat transfer to the cladding. Implementing a state-of-the-art model FGR^[20,21] should improve the simulation results.

4. In FRAPTRAN-2.0, the fuel melting was judged by a single threshold value of melting temperature. The simulation code ALCYONE provided a relatively good prediction for HBC4 and xM3,^[2] where the melting was

defined by distinct solidus and liquidus temperatures evaluated on the basis of the TAF-ID thermodynamic database.^[22] Introduction of a similar model to FRAPTRAN-2.0 should improve the simulation results.

VI. CONCLUSION

Simulations of the xM3 and HBC4 ramp tests were performed using the single-rod performance analysis codes FRAPCON and FRAPTRAN as the contribution of CRIEPI to the simulation exercise performed in P2M JEEP under the FIDES program. The conditions and assumptions used in the simulation were described in detail. The results of the simulations are summarized as follows:

1. The results of the FRAPCON simulations of base irradiation for the xM3 and HBC4 test samples reasonably agreed with the PIE data, such as fuel stack length, burnup, fluence, and oxide layer thickness on the cladding surface.
2. Using the original FRAPTRAN code, the centerline temperature during the ramp tests of xM3 and HBC4 was underestimated and the evaluated melting radius was less than the measured value.
3. A reasonable melting radius was calculated using the reduced value for gap heat conductance at the pellet-cladding interface. Validation of the modified value of the gap heat conductance was left as future work.
4. By investigating the calculated results, the limitations of FRAPTRAN-2.0 for its application to fuel melting simulations were confirmed and necessary improvements were discussed.

This study revealed the necessity of further development of models for FRAPCON and FRAPTRAN for fuel melting simulation to enable reliable simulations. The development or improvement of models for central void formation, densification, gaseous swelling and solid swelling in pellets, thermal properties of fuel in a high-temperature range, FGR, and gap heat conductance at the pellet-cladding interface are expected to be performed in a future study to reduce the uncertainty and enable the validation of fuel melting simulations.

Disclosure Statement

No potential conflict of interest was reported by the author.

ORCID

Kenta Inagaki  <http://orcid.org/0000-0003-4607-7524>

References

1. OECD/NEA, “Second Framework for Irradiation Experiments (FIDES-II),” (2022); https://www.oecd-nea.org/jcms/pl_70867/second-framework-for-irradiation-experiments-fides-ii.
2. V. D'AMBROSI et al., “P2M Simulation Exercise on Past Fuel Melting Irradiation Experiments,” *Nucl. Technol.* (2023); <https://doi.org/10.1080/00295450.2023.2194270>.
3. K. J. GEELHOOD et al., “FRAPCON-4.0: A Computer Code for the Calculation of Steady-State, Thermal-Mechanical Behavior of Oxide Fuel Rods for High Burnup,” Technical Report PNNL-19418, Vol. 1 Rev. 2, Pacific Northwest National Laboratory (2015).
4. K. J. GEELHOOD et al., “FRAPTRAN 2.0: A Computer Code for the Transient Analysis of Oxide Fuel Rods,” Technical Report PNNL-19400, Vol. 1 Rev. 2, Pacific Northwest National Laboratory (2016).
5. D. D. LANNING, C. E. BEYER, and K. J. GEELHOOD, “FRAPCON-3 Updates, Including Mixed-Oxide Fuel Properties,” Technical Report PNNL11513, Pacific Northwest National Laboratory (2005).
6. D. MANARA et al., “Melting of Stoichiometric and Hyperstoichiometric Uranium Dioxide,” *J. Nucl. Mat.*, **342**, 148 (2005); <http://dx.doi.org/10.1016/j.jnucmat.2005.04.002>.
7. W. G. LUSCHER and K. J. GEELHOOD, “Material Property Correlations: Comparisons Between FRAPCON-3.4, FRAPTRAN 1.4, and MATPRO,” PNNL-19417 NUREG/CR-7024 Pacific Northwest National Laboratory (2011).
8. B. MIHAILA, M. STAN, and J. CRAPPS, “Impact of Thermal Conductivity Models on the Coupling of Heat Transport and Oxygen Diffusion in UO₂ Nuclear Fuel Elements,” *J. Nucl. Mater.*, **430**, 221 (2012); <http://dx.doi.org/10.1016/j.jnucmat.2012.07.007>.
9. L. LEIBOWITZ et al., “Enthalpy of Liquid Uranium Dioxide to 3500 K,” *J. Nucl. Mat.*, **39**, 115 (1971); [http://dx.doi.org/10.1016/0022-3115\(71\)90190-5](http://dx.doi.org/10.1016/0022-3115(71)90190-5).
10. K. J. GEELHOOD and W. G. LUSCHER, “FRAPTRAN-2.0: Integral Assessment,” PNNL-19400 Vol. 2, Rev. 2, Pacific Northwest National Laboratory (2016).
11. L. ANDREW, “Thermomechanical Analysis of Innovative Nuclear Fuel Pin Designs,” MS Thesis, Department of Nuclear Science and Engineering, Massachusetts Institute of Technology (2010).
12. V. D'AMBROSI et al., “Presentation of the xM3 Test Case of the P2M Simulation Exercise and Modeling with the Fuel Performance Code ALCYONE,” *Nucl. Technol.* (accepted for publication); <https://doi.org/10.1080/00295450.2023.2253660>.
13. G. BONNY, “Presentation of the HBC4 Test Case of the P2M Simulation Exercise and Modeling with the Fuel Performance Code TRANSURANUS,” submitted to ANS Nuclear Technology.
14. A. TOPTAN, D. J. KROPACZEK, and M. N. AVRAMOVA, “Gap Conductance Modeling II: Optimized Model for UO₂-Zircaloy Interfaces,” *Nucl. Eng. Des.*, **355**, 110289 (2019); <http://dx.doi.org/10.1016/j.nucengdes.2019.110289>.
15. I. CLIFFORD, C. COZZO, and H. FERROUKHI, “First Assessments of the Dynamic Gap Conductance Model in TRACE,” *Proc. 18th Int. Topl. Mtg. on Nuclear Reactor Thermal Hydraulics (NURETH-18)*, p. 4624, American Nuclear Society (2019).
16. K. J. GEELHOOD, W. G. LUSCHER, and C. E. BEYER, “FRAPCON-4.0: Integral Assessment,” Vol. 2. Pacific Northwest National Laboratory (2015).
17. G. KHVOSTOV, “Modeling of Central Void Formation in LWR Fuel Pellets due to High-Temperature Restructuring,” *Nucl. Eng. Technol.*, **50**, 1190 (2018); <http://dx.doi.org/10.1016/j.net.2018.07.003>.
18. T. ARIMA, “Melting Point of Thermal Conductivity of UO₂-ZrO₂ Solid Solution: Molecular Dynamics Simulation,” *J. Comput. Chem. Jpn.*, **14-4**, 97 (2015); <http://dx.doi.org/10.2477/jccj.2015-0007>.
19. W. K. KIM, J. H. SHIM, and M. KAVIANY, “Thermophysical Properties of Liquid UO₂, ZrO₂ and Corium by Molecular Dynamics and Predictive Models,” *Trans. Korean Nuclear Society Autumn Mtg.*, Gyeongju, Korea, October 26–28, 2016 (2016).
20. G. PASTORE et al., “Modeling Fission Gas Behavior with the BISON Fuel Performance Code,” presented at the EHPG Mtg., Lillehammer, Norway, September 24–29, 2017 (2017).
21. L. C. BERNARD, J. L. JACOUD, and P. VESCO, “An Efficient Model for the Analysis of Fission Gas Release,” *J. Nucl. Mat.*, **302**, 125 (2002); [http://dx.doi.org/10.1016/S0022-3115\(02\)00793-6](http://dx.doi.org/10.1016/S0022-3115(02)00793-6).
22. A. GERMAIN et al., “Modeling High Burnup Fuel Thermochemistry, Fission Product Release and Fuel Melting During the VERDON 1 and RT6 Tests,” *J. Nucl. Mat.*, **561**, 153527 (2022); <http://dx.doi.org/10.1016/j.jnucmat.2022.153527>.